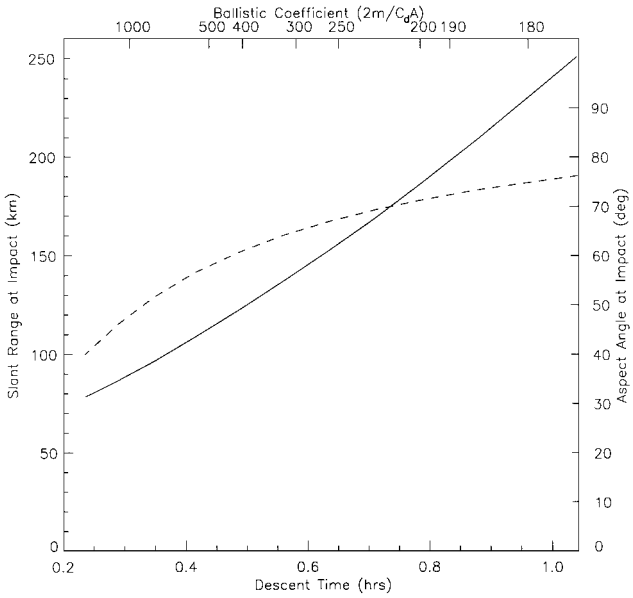

Fig. 2 Slant range (——) and aspect angle (– – –) to balloon at microprobe impact as a function of descent time and equivalent ballistic coefficient. Link geometry degrades as descent time increases.

is not compatible with a spherical geometry for these small probes. Practicable descent durations require vehicle masses of ~1 kg.

Significant mass savings are obtained by the use of advanced insulation. However, a detailed thermal analysis needs to be made to determine heat leaks through connectors, etc., because these may compromise the performance of good insulation. Similarly, if the internal power dissipation (assumed here to be 2 W, compared with typical 10- to 100-W heat leak through the insulation at impact) were to be more than a few watts, high-performance insulation would be somewhat less useful.

Phase-change materials are not mass efficient but can augment thermal margin to make a robust design (although they are no better in this respect than increasing the insulation thickness, if that is a viable option subject to the internal-power-dissipation caveat). The use of gallium (and, by implication, any mass ballast) as a phase-change material offers neither mass savings nor significant decrease in descent time because its poorer heat absorption characteristics compared with those of lithium nitrate require thicker insulation.

An increase in the packaging density of the payload itself offers substantial mass savings. Because of the mass savings (typically 25%), the denser payload does not significantly reduce the descent time.

In summary, if high-performance insulation is available and the relay link to the aerobot can tolerate ranges of 150 km and aspect angles of 70 deg, i.e., descent times of ~0.5 h, ~1-kg Venus microprobes are viable with payloads of 0.6 kg or more. Tighter relay link constraints would push to more massive probes.

Further study into Venus microprobes would require careful evaluation of the aerodynamic performance of the selected configuration (the $C_D = 0.3$ assumed here is somewhat arbitrary, and appropriate shaping of the vehicle might reduce this considerably), the relay link performance (which couples with the antenna design and the transmit power and data rate), and the thermal performance of the insulation with realistic penetrations, taking into account its nonsteady warming, i.e., its nonzero thickness. A further mission element that could be optimized is the release altitude: If the relay link is a strong driver, the aerobot might cruise at a lower altitude (where the winds are weaker and thus the range at impact will be smaller). This would permit the use of a smaller balloon because the ambient air density is higher, although the ambient temperature is also higher.

Acknowledgments

This work was supported by a contract from the Jet Propulsion Laboratory. The author acknowledges useful discussions with Jack Jones, Kerry Nock, and Jeff Hall.

References

[1]Cutts, J. A., Nock, K. T., Jones, J. A., Rodriguez, G., and Balaram, J., "Planetary Exploration by Robotic Aerovehicles," *Journal of Autonomous Robots*, Vol. 2, No. 4, 1995, pp. 261–282.

[2]Nock, K. T., Jones, J. A., and Rodriguez, G., "Planetary Aerobots: A Program for Robotic Balloon Exploration," AIAA Paper 96-0355, Jan. 1996.

[3]Heun, M. K., and Jones, J. A., "Gondola Design for Venus Deep-Atmosphere Aerobot Operations," AIAA Thermophysics Conf. (submitted).

[4]Jurgens, R. F., "High-Temperature Electronics Applications in Space Exploration," *IEEE Transactions on Industrial Electronics*, Vol. IE-29, No. 2, 1982, pp. 107–111.

[5]Schock, A., "Integration of Radioisotope Heat Source with Stirling Engine and Cooler for Venus Internal-Structure Mission," 44th Congress of the International Astronautical Federation, Paper IAF-93-R.1.426, Graz, Austria, Oct. 1993.

[6]Borucki, W. J., "Estimate of the Probability of a Lightning Strike to the Galileo Probe," *Journal of Spacecraft and Rockets*, Vol. 22, No. 2, 1985, pp. 220, 221.

[7]Lorenz, R. D., Gautier, D., and Lebreton, J.-P., "A Deep Jupiter Probe," 44th Congress of the International Astronautical Federation, Paper IAF-93-Q.5.412, Graz, Austria, Oct. 1993.

[8]Seiff, A., Schofield, J. T., Kliore, A. J., Taylor, F. W., Limaye, S. S., Revercomb, H. E., Sromovsky, L. A., Kerzhanovich, V. V., Moroz, V. I., and Marov, M. Ya., "Models of the Structure of the Atmosphere of Venus from the Surface to 100 Kilometers Altitude," *Advances in Space Research*, Vol. 5, No. 11, 1985, pp. 3–58.

[9]Kerzhanovich, V. V., and Limaye, S. S., "Circulation of the Atmosphere from the Surface to 100 km," *Advances in Space Research*, Vol. 5, No. 11, 1985, pp. 59–83.

[10]Reiss, H., "Evacuated, Load-Bearing Powder Insulation for High Temperature Applications," *Journal of Energy*, Vol. 7, No. 2, 1982, pp. 152–159.

I. E. Vas
Associate Editor

Numerical Predictions of Hypersonic Flow over a Two-Dimensional Compression Ramp

S. R. Amaratunga,* O. R. Tutty,† and G. T. Roberts‡
University of Southampton, Hampshire SO17 1BJ, England, United Kingdom

Introduction

HYPERSONIC flows over compression ramps, for example, as used for control purposes on re-entry vehicles, feature a complex structure of interacting shock waves and include shock-wave/boundary-layer interactions, which are known to induce flow separation. Subsequent flow reattachment on the ramp causes high heat fluxes, which must be predicted accurately to preserve the thermal and structural integrity of the vehicle.

Heat transfer rates from laminar, two-dimensional numerical calculations of a Mach 6.85, perfect-gas flow past a typical compression ramp are presented. Numerical results are compared with experimental data obtained from the light-piston, isentropic-compression hypersonic wind-tunnel facility at the University of Southampton.[1,2] The experimental model consisted of a flat-plate section 155 mm long followed by a ramp 51 mm long. The tunnel uses nitrogen and operates at a working-section Mach number of 6.85, a stagnation temperature ≈ 600 K, and a freestream unit $Re \approx 2.45 \times 10^6$ m^{-1}.

Presented as Paper 96-4597 at the AIAA 7th International Space Planes and Hypersonic Systems and Technologies Conference, Norfolk, VA, Nov. 18–22, 1996; received Jan. 10, 1997; revision received Nov. 29, 1997; accepted for publication Dec. 1, 1997.

*Research Student, Department of Aeronautics and Astronautics.
†Reader, Department of Aeronautics and Astronautics.
‡Senior Lecturer, Department of Aeronautics and Astronautics. Member AIAA.

These were used as the initial (freestream) conditions throughout the flow domain in the numerical model, which then was time-marched to a steady state. Ramp angles of 15, 25, and 35 deg were considered, all being well above the angle required for incipient separation.[1] Experiments were conducted with and without side plates to investigate three-dimensional (spillage) effects.

In the numerical model, the Navier–Stokes equations for a viscous compressible flow were transformed into body-fitted coordinates while the cross-derivative terms in the viscous diffusion operator were neglected. However, unlike the usual thin-layer approximations, the streamwise viscous terms were retained. The numerical scheme adopts a convection-diffusion operator splitting sequence to account for the inviscid and viscous contributions to the flow. The convection and diffusion problems are further split into systems of one-dimensional partial differential equations along grid lines. The inviscid solver is based on an explicit Harten, Lax, and van Leer (Contact) (HLLC) Riemann method; the cross-stream viscous terms are handled implicitly, whereas the streamwise viscous terms are included explicitly.

Results are presented only for the 15-deg case; further details of the numerical method and results for different ramp angles (which are broadly similar to those presented here) can be found in Ref. 3, which also describes grid refinement tests that were carried out. Note that, because of a postprocessing error, the results presented in that paper for the heat flux and the shear stress on the ramp are in error (by a factor of 2), although the values given for the flat-plate portion of the body are correct. However, neither the overall calculation procedure nor the trends exhibited were affected by this error, which now has been corrected.

Results

Density contours of the flow past the 15-deg ramp are shown in Fig. 1. Note that a length scale equal to that of the flat-plate section (155 mm) is used as a characteristic length for nondimensionalizing distances. A region of recirculation at the corner is well illustrated, as are the shock waves generated by the leading edge, the separated flow, and its subsequent reattachment on the compression ramp.

Numerical and experimental surface heat-transfer-rate distributions over the flat plate and ramp are shown in Fig. 2, presented in terms of the Stanton number

$$St = \frac{q_w}{\rho_\infty u_\infty c_{p_\infty}(T_r - T_w)}$$

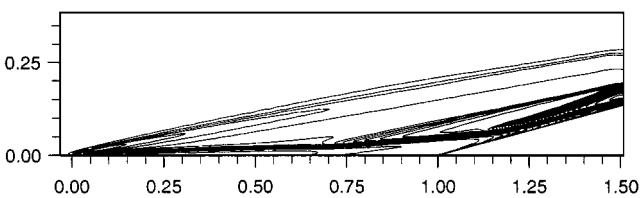

Fig. 1 Density contours for flow over 15-deg ramp. (Axes are nondimensional length scales.)

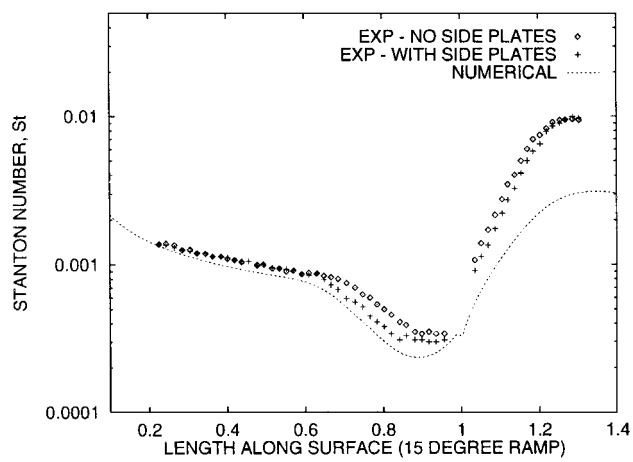

Fig. 2 Numerical and experimental surface heating rates for 15-deg ramp.

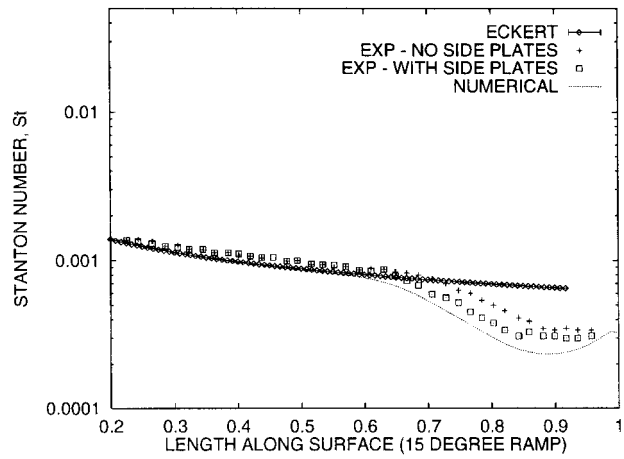

Fig. 3 Comparison of preseparated numerical and experimental flat-plate heating rates with the Eckert correlation.

where the surface heat flux is given by

$$q_w = \lambda \frac{\partial T}{\partial \eta}$$

and the recovery temperature is defined as

$$T_r = T_\infty \left\{1 + Pr^{\frac{1}{2}}[(\gamma - 1)/2]M_\infty^2\right\}$$

where λ is the gas thermal conductivity and η is the distance normal to the wall. Pr is the Prandtl number, assumed to be 0.704 for nitrogen. Subscript ∞ refers to (tunnel) freestream conditions. Other symbols have their usual meanings.

Experimental data with and without side plates, which were introduced to prevent lateral flow spillage, are shown in Fig. 2. The maximum uncertainty in the experimental heat flux data, including the effects of uncertainty in freestream conditions, has been estimated to be of the order $\pm 20\%$ (Ref. 1), although the good agreement with an empirical theory for the flat-plate flow (noted later) suggests that the uncertainty is, in fact, much less than this.

The surface heat transfer rates show flat-plate heating characteristics up to the separation point, after which there is a decrease relative to the flat-plate trend. This variation is consistent with a laminar separation.[4] The heat transfer rates on the ramp face increase steadily beyond the corner to a much higher value compared to the flat-plate heating levels, with peak heating in the reattachment area caused by boundary-layer thinning. The predicted separation and reattachment lengths are in reasonable agreement with the experimental values, though slightly overestimated, particularly at higher ramp angles.[3]

On the flat-plate section ahead of the ramp, there is a small but systematic discrepancy (within the estimated level of uncertainty) between the heat fluxes measured experimentally and those predicted by the numerical model, although the latter agree very well with results obtained using Eckert's empirical correlation[5] (Fig. 3). However, the discrepancy is much larger on the ramp, becoming worse at high ramp angles,[3] and cannot be accounted for by experimental error. Various possible reasons for this have been considered.

Lateral flow spillage from the rather low-aspect-ratio model (width/overall length ≈ 0.5) may invalidate the assumption of two-dimensional flow. In some experiments, side plates were added to contain the separated flow but, although increasing the separation and reattachment lengths and reducing the discrepancy between experimental and numerical results slightly, this did not fully resolve the observed differences. Spillage off the trailing edge of the ramp (with consequent boundary-layer thinning) also was considered, and the numerical model was refined by adding a second (sharp) corner to the grid at the location corresponding to the trailing edge of the experimental model. However, although the heat fluxes were increased near the corner, the effect was found to be very localized, and elsewhere the overall agreement between experiment and prediction was not significantly improved.[3]

As described earlier, the reduction in heating at separation indicates that the flow remains laminar up to that point; however, it is well known that separated flows are particularly prone to transition in the shear layer.[6] In this case, transition is most likely at the higher flap angles and could reduce the separation length while substantially increasing the heat flux at reattachment.[7] Transition therefore could help explain the observed discrepancies between experimental results and numerical predictions. Similarly, the presence of Görtler-like vortical structures in the reattachment zone also must be considered a possibility. Evidence for such structures, both in the initially laminar interactions reported here and in higher-Reynolds-number flows where the interaction is known to be turbulent, has been obtained in experiments involving liquid crystal thermography.[1,8] The observed spacing of these structures was such that it is quite possible that at least one crossed each gauge in this region, causing an increase in the local heat flux.

In an attempt to resolve these differences, numerical modeling of this type of flowfield at a higher Mach number and a lower unit Reynolds number[9] was carried out. Under these conditions, the flowfield is more likely to remain laminar and free from three-dimensional effects. The preliminary results obtained (not reported here) were compared with experimental and computational results reported in Ref. 9. In this case, our numerical results slightly overpredict the experimental heat fluxes but agree well with the other computational results, supporting our view that unaccounted-for three-dimensional and/or transition effects were present in the Southampton experiments. Further developments of the code are being planned to allow the investigation of flowfields involving these phenomena as well as other, more complex, three-dimensional features in hypersonic flows.

Conclusions

Numerical simulations of a laminar, two-dimensional flat-plate/compression-ramp hypersonic flow have been carried out. It appears that the general flow features, which include a large region of separated flow, are modeled correctly but the separation and reattachment lengths are slightly overpredicted. Although good agreement with experimental heat flux data is apparent on the flat-plate surface, the heat flux is underpredicted on the ramp and, in particular, in the reattachment area. Reasons for the discrepancies are discussed, and it is concluded that three-dimensional effects, possibly accompanied by transition in the free shear layer, are probably responsible for the observed differences between numerical and experimental results.

Acknowledgments

This work was supported by the United Kingdom Engineering and Physical Science Research Council. R. A. East of the Department of Aeronautics and Astronautics, University of Southampton, and P. Batten of the University of Manchester Institute of Science and Technology are thanked for their advice.

References

[1]Smith, A. J. D., "The Dynamic Response of a Wedge Separated Hypersonic Flow and Its Effects on Heat Transfer," Ph.D. Thesis, Dept. of Aeronautics and Astronautics, Univ. of Southampton, Southampton, England, UK, 1993.

[2]Smith, A. J. D., and East, R. A., "Interference and Transient Effects on Compression Ramp Flows at Hypersonic Mach Numbers," *Shock Waves @ Marseille, Proceedings of the 19th International Symposium on Shock Waves*, edited by R. Brun and L. Z. Dumitrescu, Vol. 1, Springer–Verlag, Berlin, 1995, pp. 41–46.

[3]Amaratunga, S. R., Tutty, O. R., and Roberts, G. T., "Numerical Predictions of Hypersonic Flow Past a Body/Body-Flap Configuration," AIAA Paper 96-4587, Nov. 1996.

[4]Holden, M. S., "Boundary-Layer Displacement and Leading-Edge Bluntness Effects on Attached and Separated Laminar Boundary Layers in a Compression Corner, Part II: Experimental Study," *AIAA Journal*, Vol. 9, No. 1, 1971, pp. 84–93.

[5]Eckert, E. R. G., "Engineering Relations for Skin Friction and Heat Transfer to Surfaces in High Velocity Flows," *Journal of the Aerospace Sciences*, Vol. 22, Aug. 1955, pp. 585–587.

[6]Johnson, C. B., "Heat Transfer Measurements at Mach 8 on a Flat Plate with Deflected Trailing-Edge Flap with Effects of Transition Included," NASA TN-D5899, 1970.

[7]Simeonides, G., and Haase, W., "Experimental and Computational Investigations of Hypersonic Flow About Compression Ramps," *Journal of Fluid Mechanics*, Vol. 283, Jan. 1995, pp. 17–42.

[8]East, R. A., and Smith, A. J. D., "Unsteadiness in Separated Hypersonic Flows," Dept. of Aeronautics and Astronautics, CR RDMF/E 14/87, Univ. of Southampton, Southampton, England, UK, May 1992.

[9]Grasso, F., and Marini, M., "Hypersonic Shock-Wave Laminar Boundary Layer Interaction," *Computers and Fluids*, Vol. 25, No. 6, 1996, pp. 561–581.

J. R. Maus
Associate Editor

Greatest Critical Difference Statistics in *k*-out-of-*n* Reliability Structures

Hüseyin Sarper,* and Roger W. Johnson†
University of Southern Colorado, Pueblo, Colorado 81001
and
Phermsak Siriphala‡
Wichita State University, Wichita, Kansas 67208

Introduction

As the new millennium approaches, there is increasing expectation that routine but limited space travel will be a reality. Travel beyond the solar system is likely to remain for now a very distant idea due to the well-known physical laws or the way such laws are understood at this time. Regardless of the nature of space travel, risk is a fundamental consideration. There is often a negative relationship between the cost and the risks of the mission. If sufficient risk is accepted, a mission may cost a fraction of the amount needed for a much less risky one. As travel distances get larger, risk analysis becomes even more relevant. A new probability tool, distribution of the greatest critical difference of component lives or simply the range distribution, is suggested, possibly for the first time in reliability literature. This study considers a reliability concern of spacecraft, given that each of their engines has a life that is a random variable with known or estimated parameters. If each engine has a random life at some specified operating conditions, such as speed and temperature, then the probability of failure and the failure rate will increase over time in the absence of preventive maintenance. Decision makers can install a fixed number n of such engines, some or all of which are needed to keep the spacecraft flying. Assume that it is possible to keep the spacecraft flying if one or more of the engines have failed. The proposed methodology can be applied to spacecraft structure scenarios in various decision stages, especially, for example, the prephase A stage used in NASA's decision process. In a 4-out-of-4 system (where all engines must be operable for the spacecraft to fly), the system life distribution is the same as the distribution of the minimum life component. On the other hand, the 1-out-of-4 system (where only one engine is required to power the spacecraft) has a life distribution that is the same as the distribution of the maximum life component. Sarper[1] has shown analytical and simulation results for the distribution of the extremes in the four-engine case. This study shows analytical solutions for range analysis using the 1-out-of-4 case. Then simulation is used and is validated against the analytical solution. This validation is used in suggesting that simulation-only results for other cases should be valid too.

Received June 27, 1997; revision received Dec. 4, 1997; accepted for publication Dec. 4, 1997.

*Associate Professor of Engineering, 2200 Bonforte Boulevard. E-mail: sarper@uscolo.edu.

†Professor of Mathematics, 2200 Bonforte Boulevard.

‡Graduate Student, Department of Industrial Engineering.